Title
OPERATION OF THE 88-INCH CYCLOTRON

Authors
Grunder, Hermann
Selph, Frank.

Publication Date
1964-04-01

UCRL-11477 (corrected) + (errata 11-4-65) + errata 4-18-66

University of California

Ernest O. Lawrence Radiation Laboratory

OPERATION OF THE 88-INCH CYCLOTRON

DISCLAIMER

UNIVERSITY OF CALIFORNIA

Lawrence Radiation Laboratory
Berkeley, California

AEC Contract No. W-7405-eng-48

September 30, 1964

ERRATUM

TO: All recipients of UCRL-11477

FROM: Technical Information Division

SUBJECT: UCRL-11477, "Operation of the 88-Inch Cyclotron," by Hermann Grunder and Frank Selph. April 1964.

This Completed

Please replace pages 11 and 12 with attached corrected page. Figure 8 has the correction on it. Figure 9 remains the same.

UNIVERSITY OF CALIFORNIA

Lawrence Radiation Laboratory
Berkeley, California

AEC Contract No. W-7405-eng-48

November 4, 1965

ERRATA

TO: All recipients of UCRL-11477

FROM: Technical Information Division

SUBJECT: UCRL-11477, "Operation of the 88-Inch Cyclotron," by Hermann Grunder and Frank Selph. April 1964.

Page	Line	Correction
5	Fig. 3	The beam-intensity distributions shown should be corrected for the factors listed on corrected page 6, lines 6 through 11, for one to get a true picture of I vs sin ϕ.
6	Lines 6-11	Should read: By differentiation of the fall-off between A and B, the beam-intensity distribution can be obtained [Fig. 3 (c)]. The ordinates on this curve should be corrected for variations in slope of the sin ϕ vs radius curve, and for variation in the particle turn density with radius. This correction converts dI/dR to dI/d(sin ϕ). The abscissa values should also be converted from radius to sin ϕ dependence by the above factors. These corrections would then give an I vs sin ϕ curve which is independent of the cross section taken.
7	Fig. 4	The beam-intensity distributions should be corrected as for page 5, figure 3, above.

DAVID J. CLARK

UNIVERSITY OF CALIFORNIA
Lawrence Radiation Laboratory
Berkeley, California

AEC Contract No. W-7405-eng-48

April 18, 1966

ERRATA

TO: All recipients of UCRL-11477

FROM: Technical Information Division

SUBJECT: UCRL-11477, "Operation of the 88-Inch Cyclotron," by Hermann Grunder and Frank Selph. April 1964.

The following is to be added for page 6, lines 6-11.

The factor to be used in the corrections is $\Delta S = \Delta S_{\Delta B} + \Delta S_{\Delta f}$. $\Delta S_{\Delta B}$ is the rate of change of sin ϕ with radius with $\Delta f = 0$. It is a measure of how far from isochronism the magnetic field is. $\Delta S_{\Delta f}$ is the rate of change of sin ϕ with radius due to the detuning, Δf. It is approximately equal to $4\pi \frac{\Delta f}{f} N_t \frac{r}{r_m^2}$ nonrelativistically, where N_t is the total number of turns in the cyclotron at full energy gain, and r_m is the radius for the N_t turns. To make the corrections to the curves, one should divide dI/dR by ΔS to get dI/d sin ϕ. To get an abscissa proportional to sin ϕ, one should multiply the radial intervals by ΔS: $\Delta \sin \phi = \Delta S \times \Delta r$.

A direct method can also be used for finding the beam phase distribution. If one measures beam current, I, vs Δf at a fixed radius, one can then get I vs sin ϕ from the linear relation between sin ϕ and Δf. Approximately: $\Delta \sin \phi = 2\pi \frac{\Delta f}{f} N_t \frac{r^2}{r_m^2}$. One can check that the beam is not being cut off at a smaller radius by using both positive and negative Δf runs, or several radii, to check consistency.

David J. Clark

Presented at the APS Meeting-April 1964

UCRL-11477 corrected

UNIVERSITY OF CALIFORNIA
Lawrence Radiation Laboratory
Berkeley, California

AEC Contract No. W-7405-eng-48

OPERATION OF THE 88-INCH CYCLOTRON

Hermann Grunder and Frank Selph

April 1964

OPERATION OF THE 88-INCH CYCLOTRON*

Hermann Grunder and Frank Selph

Lawrence Radiation Laboratory
University of California
Berkeley, California

April 1964

ABSTRACT

Experimental facilities at the 88-inch Cyclotron as of May 1964 are briefly discussed. Characteristics of the beams are described, including intensity as a function of time, radial and vertical source positions, and emittance and the energy spread. Some data are presented on the distribution of machine time and on the availability of beams.

---

*Paper submitted to the April, 1964 Meeting of the American Physical Society.

EXPERIMENTAL LAYOUT

There are presently proton beams from 10 to 50 MeV, alpha beams from 25 to 135 MeV, and deuteron beams from 12.5 to 67 MeV available for the experimenter. Figure 1 shows the layout of the 88-inch experimental setup. From the experimenter's viewpoint the cyclotron can be reduced to the two effective sources in the radial and vertical planes, respectively. Knowing the characteristics of these sources and their positions relative to the optical axis of the first quadrupole, one can guide the beam by the switching magnet into any one of five experimental setups.

First, the High-Level Cave (HLC), which is used for radioisotope production or for experiments that endanger the experimental area because of radioactive contamination. The optical system for the High-Level Cave was designed by Hugo Atterling of Stockholm in such a way that dispersion of fringe fields, switching magnet, and bending magnet cancel, and the beam is essentially undispersed as it arrives at the target.

Cave 1 has been designed for good energy analysis, and the energy resolution $\Delta E/E$ of 0.15% (including counter and electronic errors) has been attained. The beam intensity is reduced by about a factor of 25. There is an analyzing slit positioned inside the vault to reduce the background in the cave. All experiments performed in Cave 1 make use of scattering chambers in one way or another.

The same statements are true for Cave 2, where an energy resolution of the same order can be reached.

Cave 3 has up to now an essentially undispersed beam, and has been used for biomedical purposes or scattering experiments which don't require an energy resolution $\Delta E/E$ of better than 0.5%, which is in fact the energy spread of the whole beam.

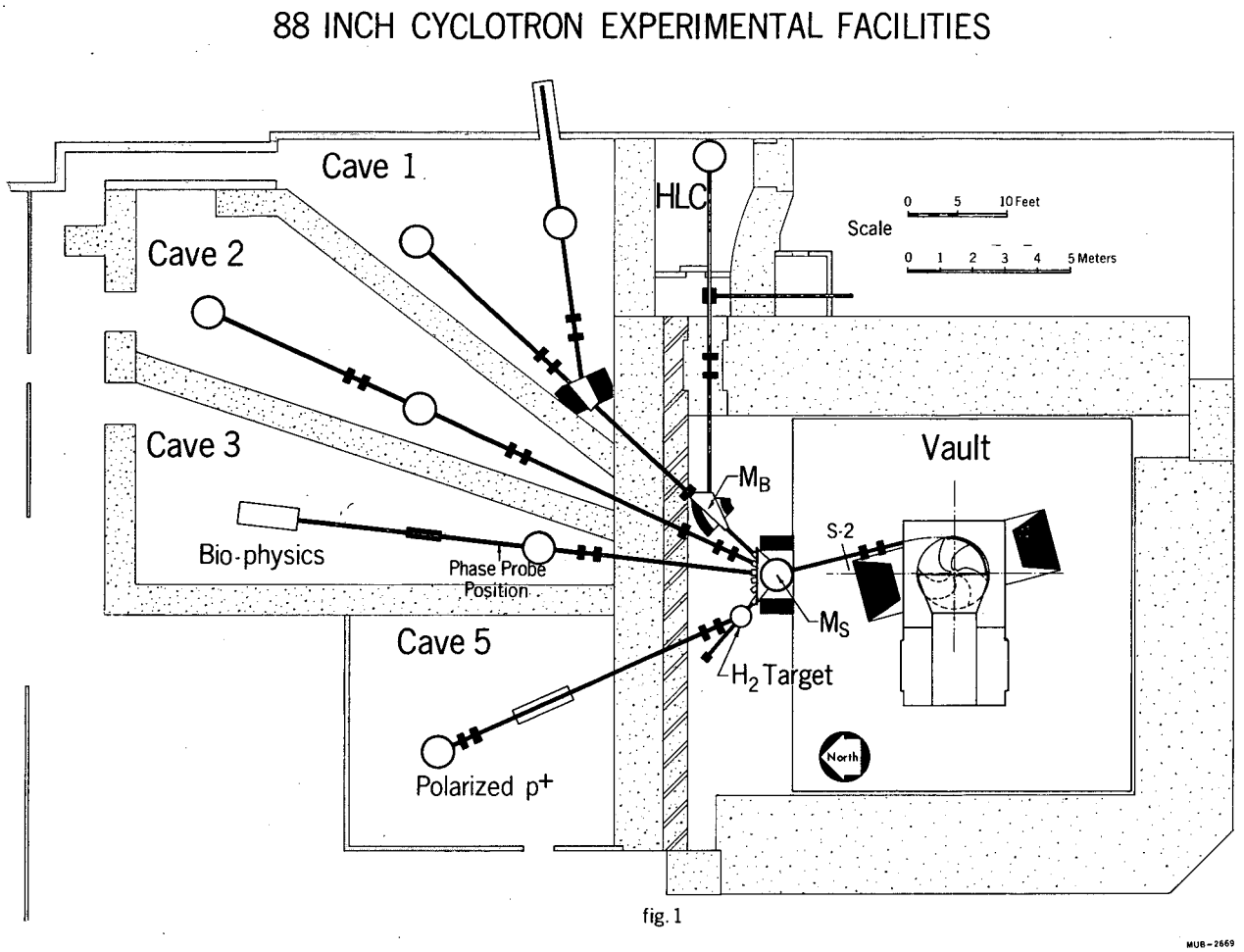

Fig. 1. 88-Inch cyclotron experimental facilities.

Cave 5 is used for experiments with polarized protons produced by an incident alpha beam on a hydrogen target.

BEAM CHARACTERISTICS--GENERAL

The primary interest of an experimenter is in beam quantity and quality. The beam is described by:

(a) The intensity as a function of time.

(b) The effective source position, source width, angular divergence, and density distribution in the horizontal and vertical planes.

(c) The energy and energy spread.

Since the beam quality is determined by the properties of the internal beam, it is necessary to have knowledge of the internal beam behavior.

The Berkeley-88-inch cyclotron is a three-sector-spiral ridge machine, with a single dee. A plan view of the pole tip is given in Fig. 2.

BEAM CHARACTERISTICS--INTERNAL

Much useful information about the internal beam behavior can be deduced from a current-vs-radius diagram (Fig. 3b). The beam can be lost before it reaches extraction radius either because of insufficient vertical focusing or because of shift in phase relative to the rf of $\pm 90°$. On the basis of this phase shift, Alper Garren and Lloyd Smith have shown how to construct a diagram showing the phase of the beam as a function of radius.[1] One first obtains an I-vs-R record at a frequency f_0. Then a deliberate frequency error Δf is induced, leaving all other machine parameters constant. A decreased frequency $f_0 - \Delta f$ causes the beam to lead the rf until $\sin \phi$ becomes 1 and further acceleration is impossible (Fig. 3a). The beginning

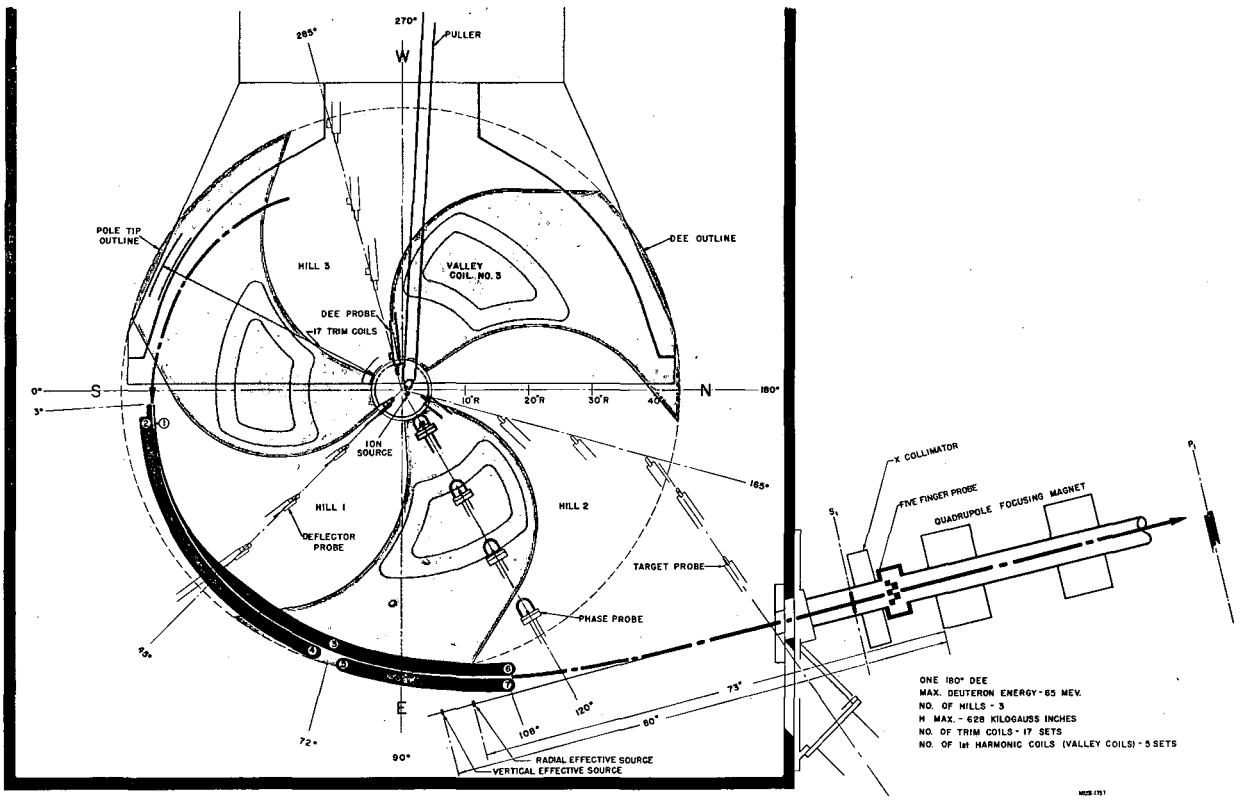

fig. 2

Fig. 2. 88-Inch cyclotron pole tip.

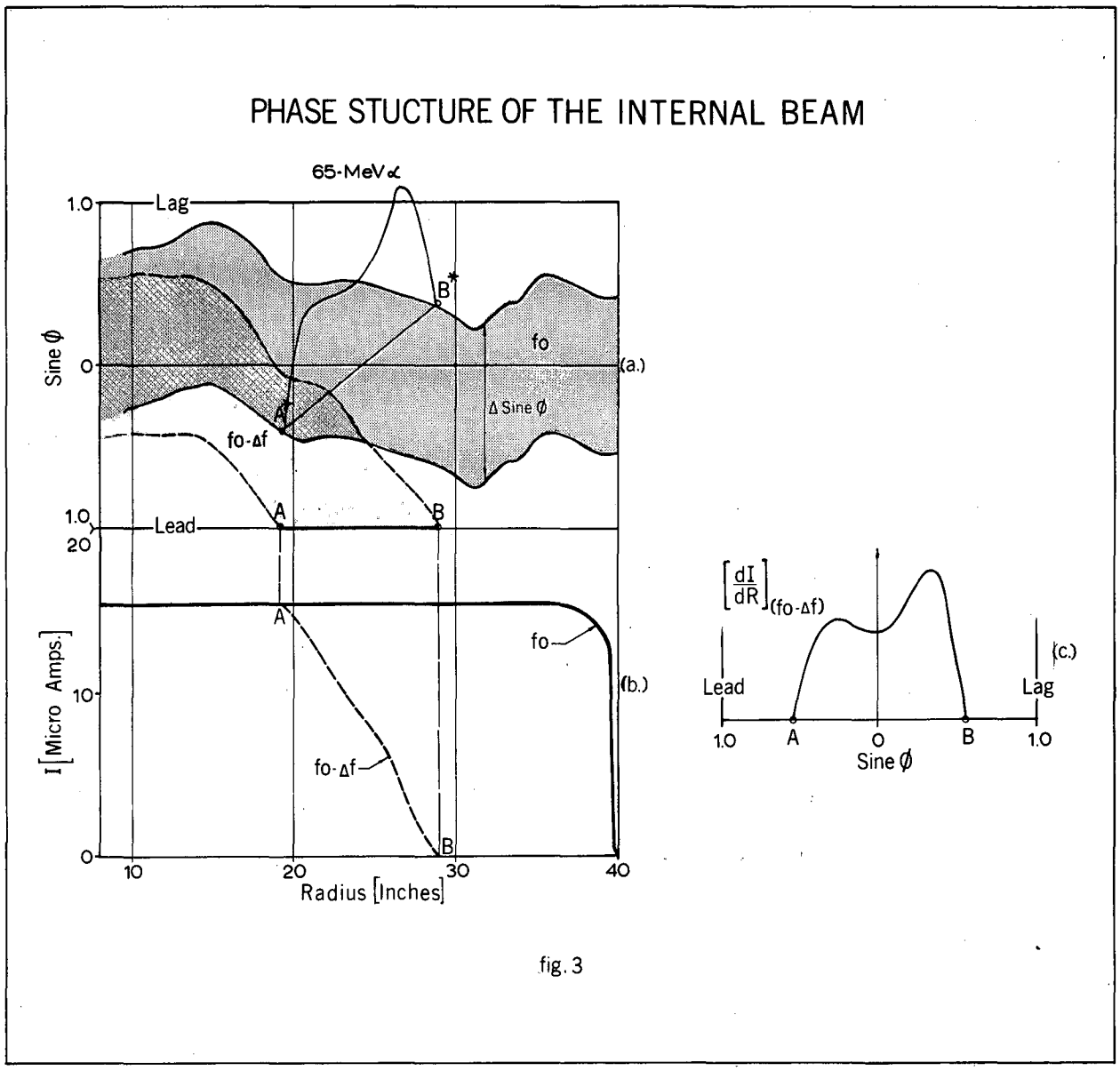

fig. 3

MUB-2668

Fig. 3. Phase structure of the internal beam.

and end of the loss of this beam can be easily established with its I vs R (Points A, B) for ($f_0 - \Delta f$). By calculating the phase shift due to the frequency error $-\Delta f$, the points A^*, B^* on the phase-shift diagram drawn for f_0 are established. The procedure is repeated for several lower frequencies to obtain the full curve.

By differentiating the fall-off between A and B, the beam intensity distribution vs phase can be obtained (Fig. 3c). Point A is lagging in time behind the peak of rf voltage, whereas B is leading. The lagging part of the beam is consistently more intense than the leading part for all energies. The reason for this phenomenon is probably the favorable vertical electrostatic focusing in the first few turns.

Figure 4 shows the phase-shift diagram and the beam-intensity distribution vs phase of a low- and a high-energy alpha beam. With our present ion source and center region arrangement, the phase width of the internal beam is a maximum at the low-energy beams ($\Delta \sin\phi \approx 1$) and a minimum at the high energies ($\Delta \sin\phi \approx 0.6$). The phase-vs-radius diagrams are reproducible and known for the 88-inch in 5-MeV steps.

BEAM CHARACTERISTICS: EXTERNAL--PHASE WIDTH

The deflection of the beam is by means of two electrostatic deflector channels. The necessary gradients are 60 to 150 kV/cm, depending on energy. The beam current vs phase of the external beam has been measured for various energies, by use of diffused silicon detectors with oxide-projected junction edges[2] 0.010 in. thick directly in the beam. A 10-volt signal can readily be obtained from this counter and fed directly to a Tektronix 519 oscilloscope, giving a total rise time of less than 2 nanoseconds. The probe assembly is shown in Figs. 5 and 6. To protect the crystal from heat damage

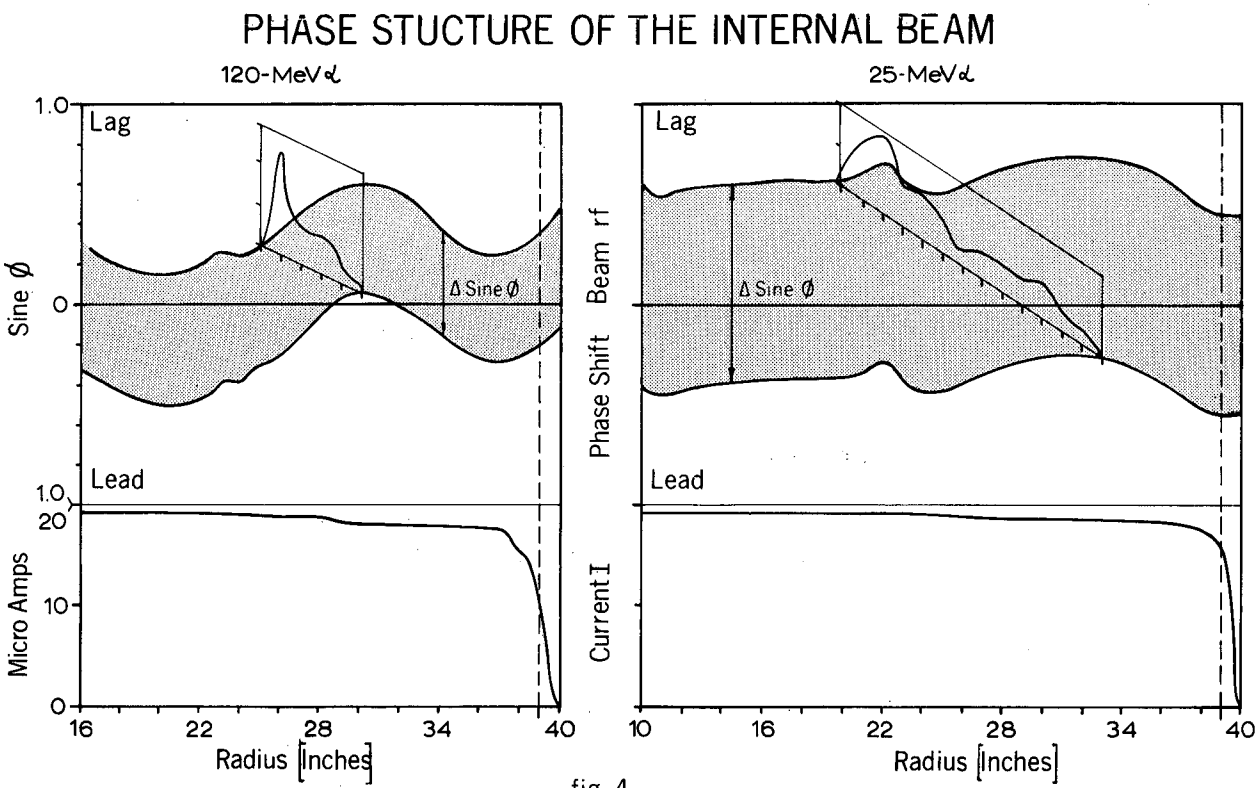

fig. 4

Fig. 4. Phase structure of the internal beam.

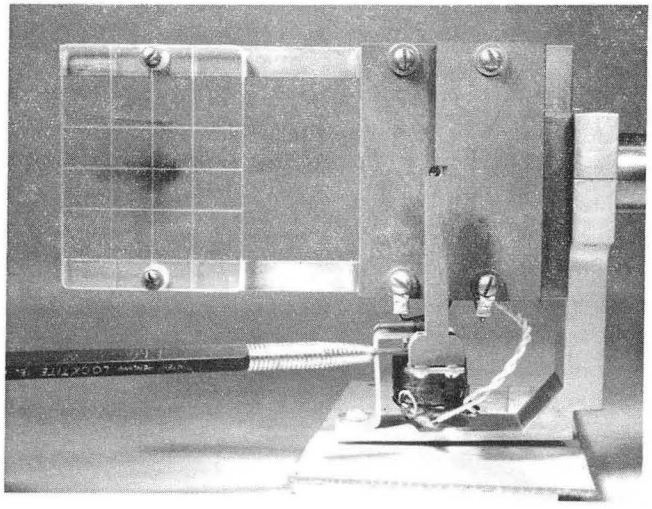

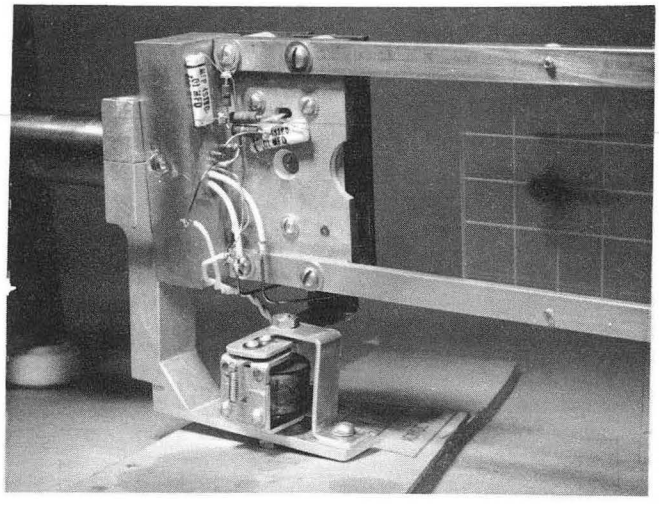

ZN-4329

Fig. 5. Front view of external phase probe.

Fig. 6. Rear view of external phase probe.

a solenoid-actuated shutter is placed immediately in front of the detector. Bursts of a few milliseconds' duration are allowed to strike the detector every few seconds.

The center trace in Fig. 7 shows the current vs time for the normal running condition (frequency f_0) of a 65-MeV alpha beam. There is a main peak of beam and a shoulder on the leading side of the pulse. The phase width, discounting the tail on the lagging side of the pulse, has been measured as 16×10^{-9} sec, or 52°. This is about 2/3 of the internal phase width.

On introduction of a small frequency error, the current-vs-time pulse ought to change, because the current distribution over the internal phase width is not a constant as shown in Figs. 3 and 4, and different parts of the internal beam will be lost in phase.

A negative frequency error Δf favors the lagging part of the internal beam, which is more intense. Conversely, a positive frequency error favors the leading part of the beam, which is less intense. A further increased frequency error narrows the phase width until the external beam vanishes. Figure 8 shows the comparable photograph for the 80-MeV alpha beam.

Figure 9 shows, twice, a succession of about 60 pulses of 80-MeV alpha particles with a 1.7-second interval between them. The frequency $f_0 - \Delta f$ produces a very stable beam, whereas a slightly higher frequency than f_0 appears to have an intensity change which is modulated with a frequency of ≈ 0.5 Mc/sec. The center frequency f_0 seems to be a combination of both extreme components. This is in good agreement with the intensity distribution of the single pulse (Fig. 8).

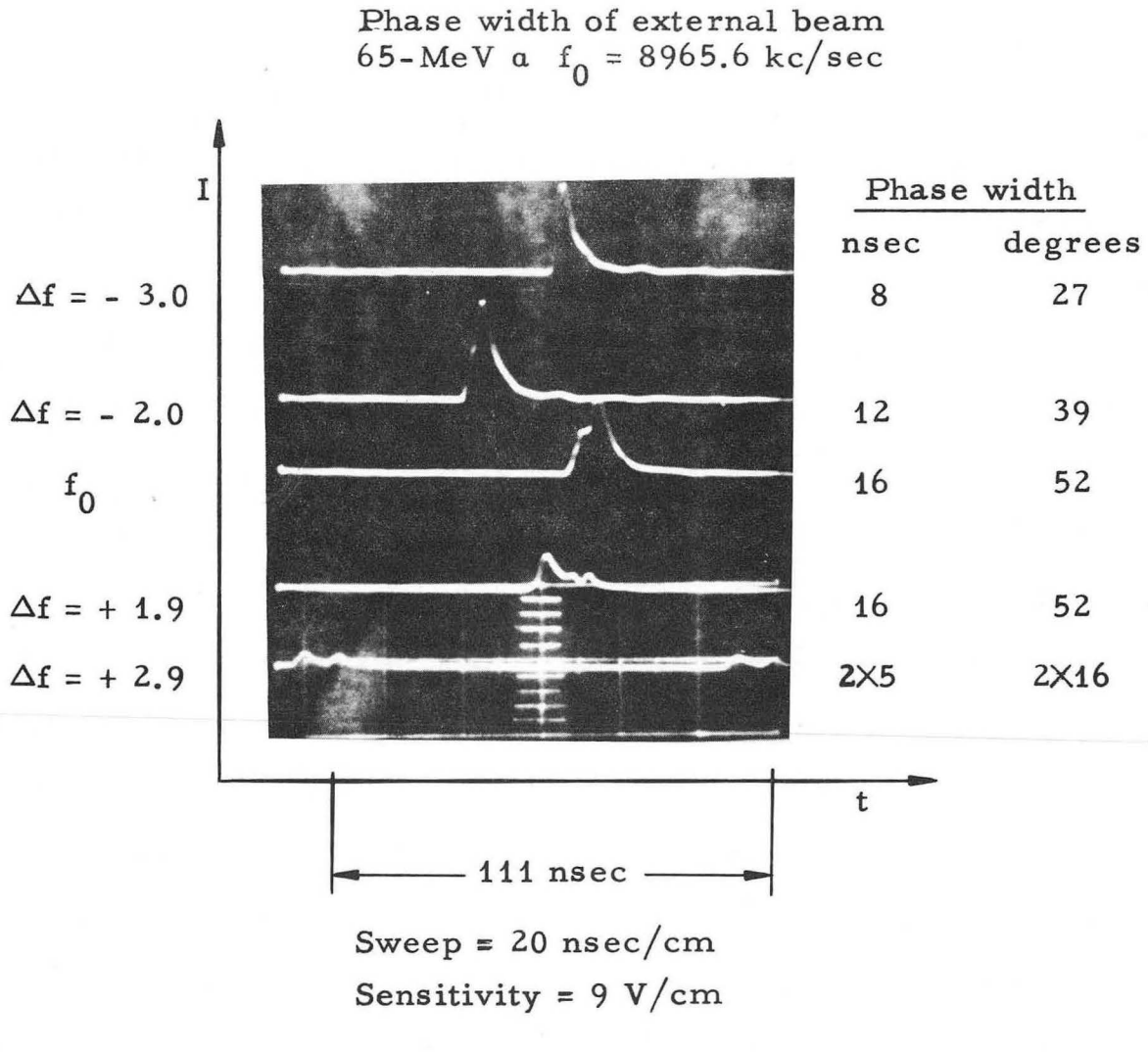

Fig. 7. Phase width of external beam.
65-MeV α; f_0 = 8965.6 kc/sec. Sweep = 20 nsec/cm, sensitivity = 9V/cm.

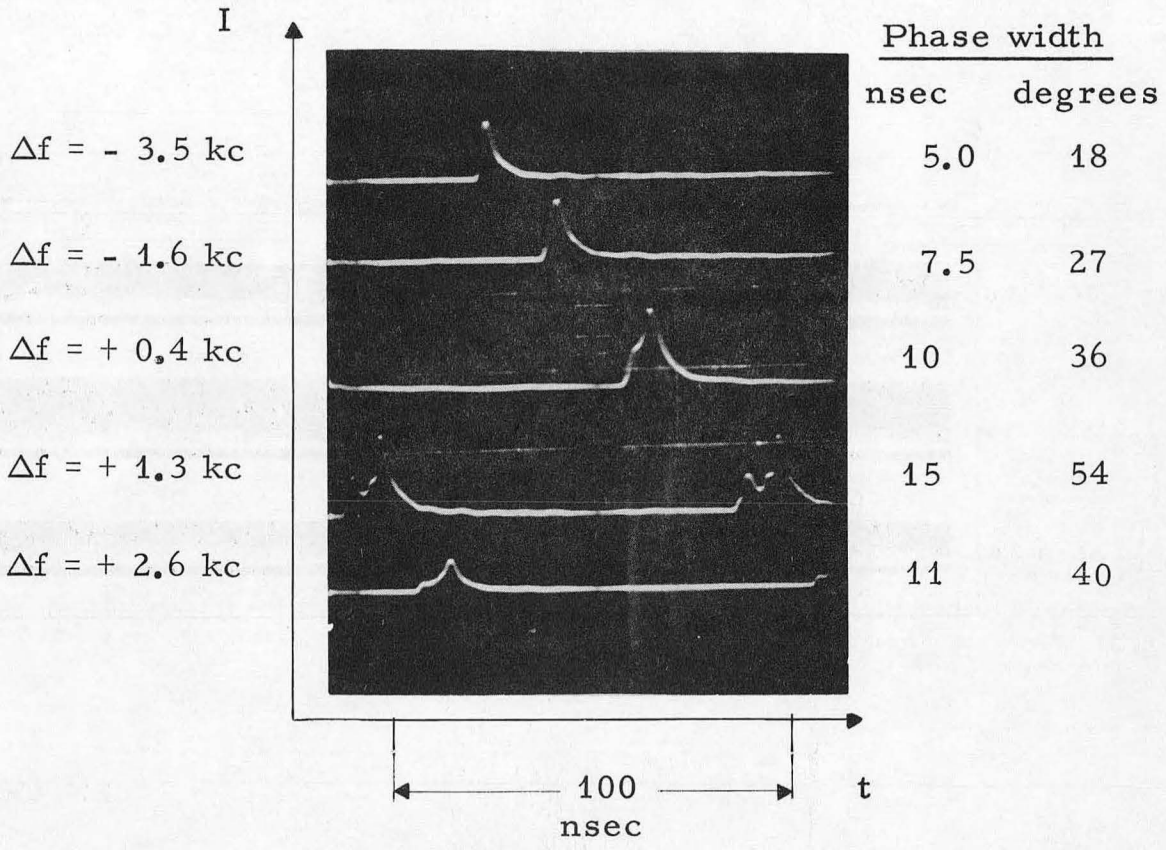

Fig. 8. Pulse width of external beam.
80-MeV α; f_0 = 9986.6 kc/sec.

This is correct page , per erratum dated 9-30-64

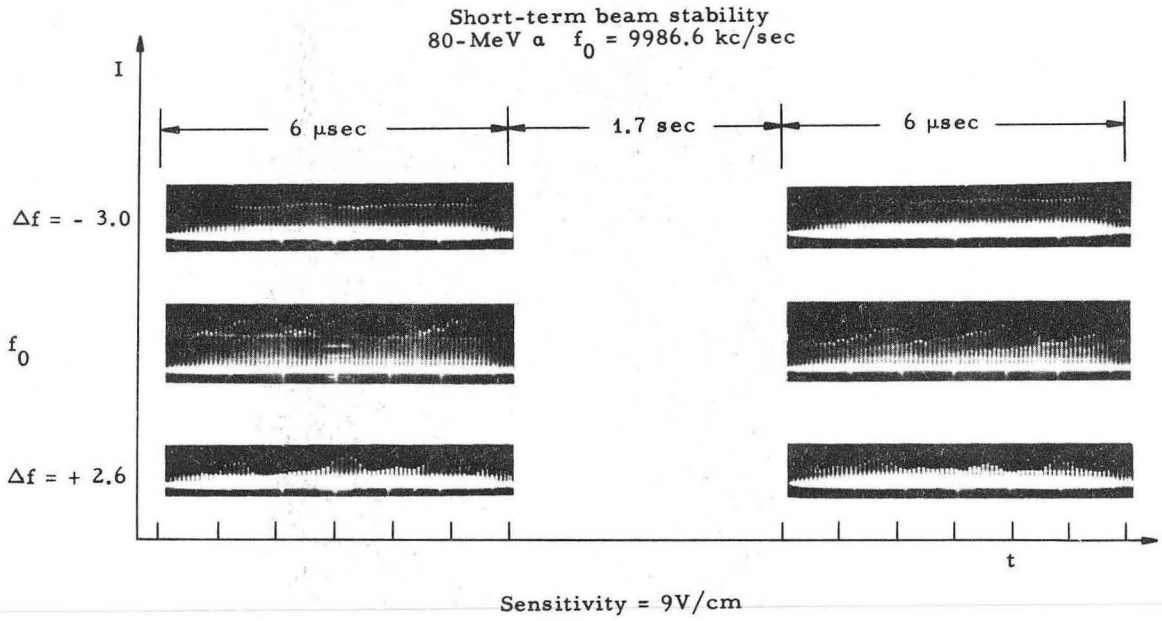

ZN-4332

Fig. 9. Short-term beam stability.
80-MeV α; f_0 = 9986.6 kc/sec. Sweep = 20 nsec/cm, sensitivity = 9V/cm.

this page correct per erratum , 9-30-64

RADIAL SOURCE

The radial effective source in the 88-inch cyclotron is about 72 inches upstream of the effective edge of the first quadrupole.[3] Different particles and energies show a spread of the source position transversely as well as longitudinally. Figure 10 shows the radial effective source positions relative to the effective edge of the first quadrupole (longitudinally) and relative to the axis of the beam pipe. The effective sources of all beams have a spread of 1.2 in. transversely, with a longitudinal variation of 4 in. The reproducibility of the source position is within ±0.05 in. transversely and 1 in. longitudinally. This reproducibility is essential for an effective beam transport system. The optical axis of the first quadrupole doublet is aligned so that all beams can be used effectively for experiments. An improved support now being designed will permit rotation of the first quadrupole around the center of the switching magnet in the radial plane, bringing the radial effective source for all beams onto the optical axis, so that all beams will have normal entry into the switching magnet, and the beam position at the target will be independent of particle and energy.

In Fig. 10, the effective source is assumed to be a point source. This is an adequate assumption for beam-transport purposes. In predicting beam sizes at focal points, however, the assumption of a point source is insufficient.

A more detailed knowledge of the source characteristics can be obtained by measuring the emittance of the source.[3] The emittance is defined here as the area occupied by the beam in a space with the coordinates x (transverse position) and $\alpha \approx p_x/p$, where p is the momentum of the particle and p_x is the transverse momentum.

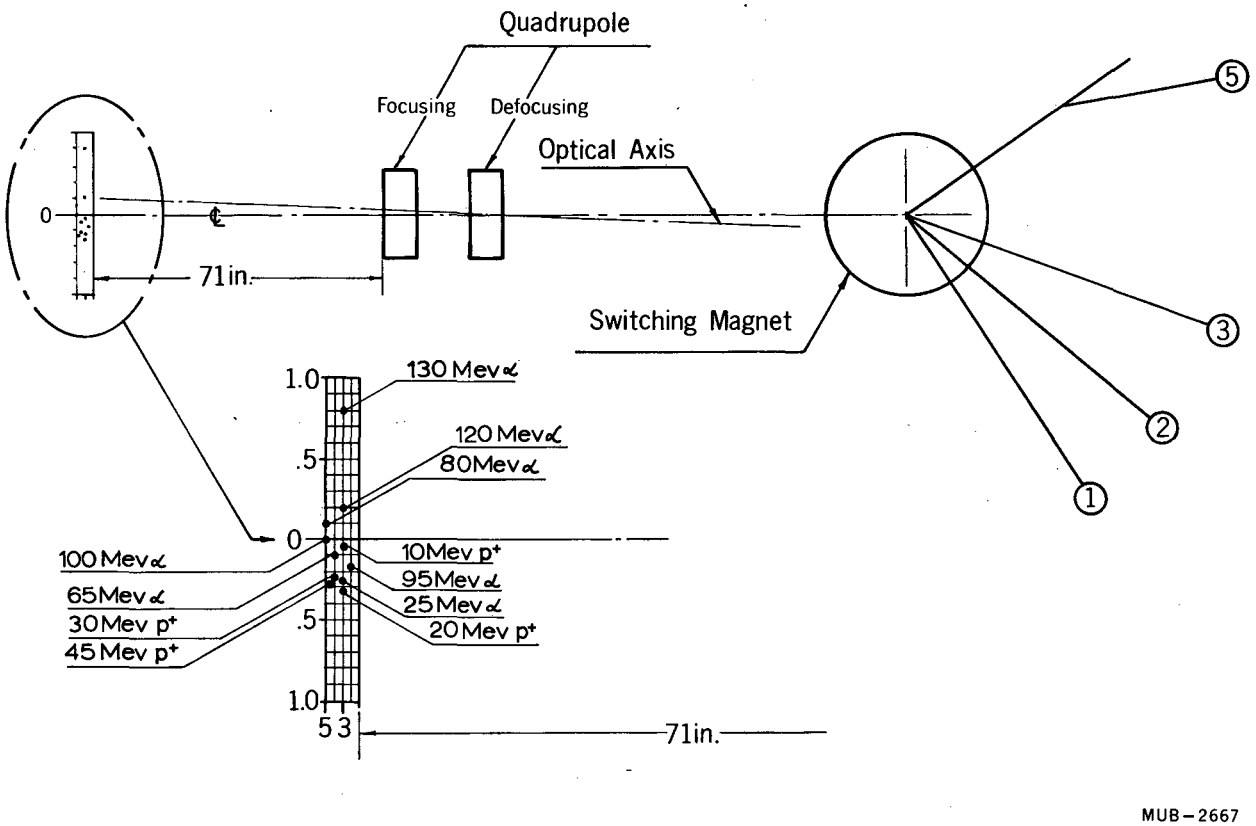

Fig. 10. Radial effective source position.

The radial emittances of the 88-inch cyclotron are identical, within the accuracy of the measurements, over the whole energy range (Fig. 11).

Since many experiments can accept only a limited angular divergence, the beam intensity distribution vs angle has been measured (Fig. 11). Here again within the accuracy of the measurment there is no difference between various beams. The linear density distribution is somewhat surprising.

BEAM ANALYSIS

The present beam-analyzing system makes use of the switching magnet needed inherently to transport the beam into Cave 1. The system was laid out by Hugo Atterling in cooperation with Bernard Harvey. The intent is to add, to the dispersion of the fringe field of the cyclotron, the dispersion of the switching magnet.

We have in a qualitative way verified that in fact the two dispersions will be added. In addition we have measured the energy spread $\Delta E/E$ of the uncollimated beam. For 95% of the beam the energy resolution becomes $(\Delta E/E)_{95\%} \approx 0.9\%$, whereas the full width of the energy spread at half maximum becomes $\Delta E/E \approx 0.5\%$. These measurements have been done repeatedly with 33-MeV alphas. Check points indicate that no drastic changes are to be expected for other energies. As mentioned earlier, the analyzed beam energy spread, full width at half maximum, is $\Delta E/E = 0.15\%$.

The beam intensity distribution vs energy (Fig. 12) shows a strong peak on the high-energy side of the beam. Most of the beam appears to have an energy close to E_0. Nevertheless, the "low-energy tail" $E_0 - \Delta E$ exists, and causes us difficulty in the energy analysis.

A quantitative feeling for the energy analysis in the fringe field can be obtained by inserting a 0.010-in. slit (S2) at the first focal point. The

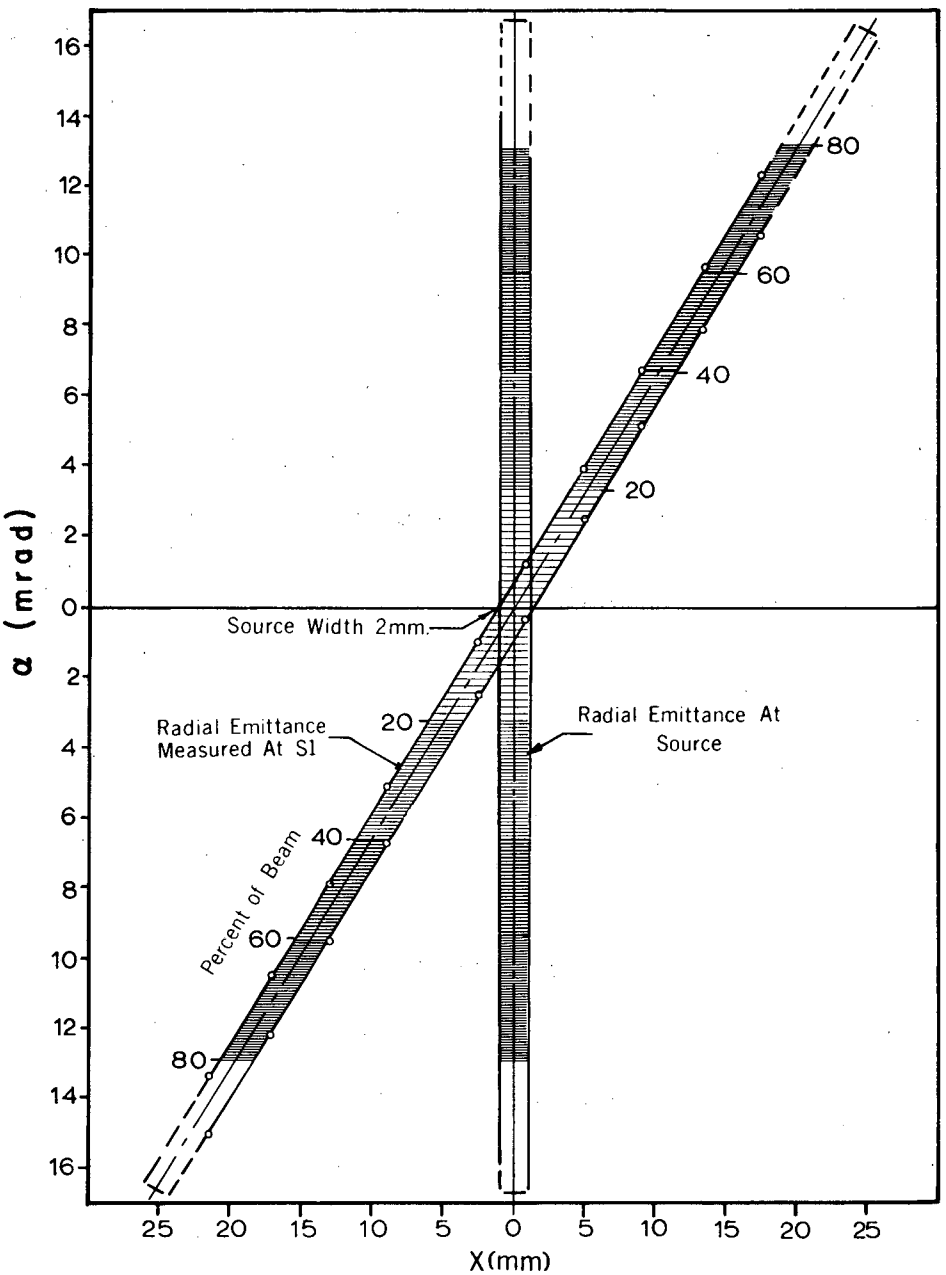

Fig. 11. Radial emittance, 60 mm mr.

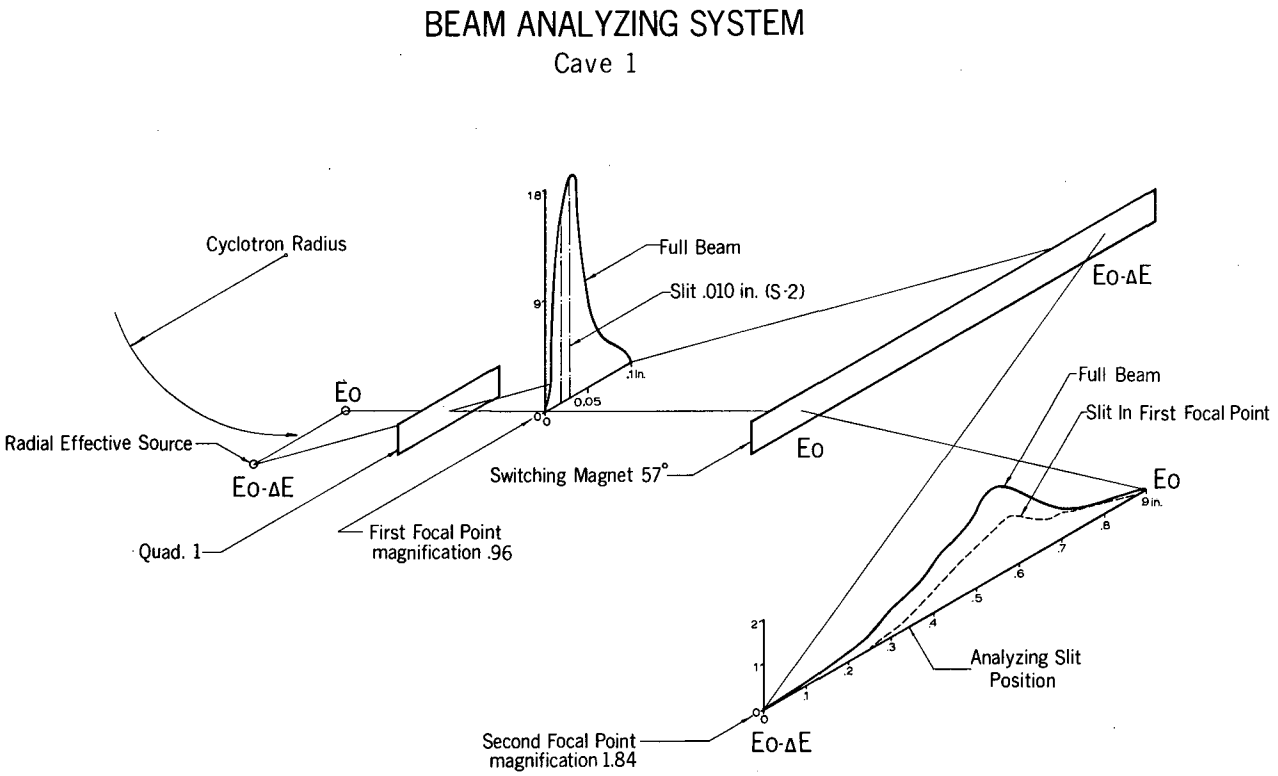

fig. 12

Fig. 12. Beam-analyzing system, Cave 1.

beam image produced at the second focal point is shown in Fig. 12. A selected beam of 20% of the full intensity reduces the energy spread to $(\Delta E/E)_{20\%} = 0.7\%$.

VERTICAL SOURCE

The vertical plane is less well understood than the radial plane. We have some knowledge of the vertical beam height of the internal beam near extraction radius. Figure 13 shows foils which were inserted into the beam to indicate beam position by the burn pattern. We do not understand yet why the beam is high, particularly at 36 inches. The effect of beam "blow-up" due to the coupling resonance ($2\nu_z = \nu_r$, where twice the vertical betatron oscillation frequency equals the radial betatron oscillation frequency), is quite distinctly visible at all energies. The strong vertical focusing compresses the beam vertically at extraction radius (39 inches) to such an extent that it can give rise to damage on the high-voltage electrode of the deflector.

Vertical effective-source measurements have been done and indicate the source position $\approx$ 80 inches upstream of the effective pole edge of the first quadrupole. The divergence in the vertical plane is small, 3.3×10^{-3} radians, making accurate source measurements difficult. The vertical emittance is of the same order as the radial emittance.

PRESENT STATUS OF OPERATION

The current of the external beam is restricted by heating of the septum that divides the internal from the external beam, and is part of the ground electrode of the first deflector channel. The power limitation is approximately 2 kW internal beam, which represents about 700 watts external beam. This is about 20 μA of 65-MeV alphas. The present septum is made out of tungsten and is uncooled. A water-cooled septum was placed in

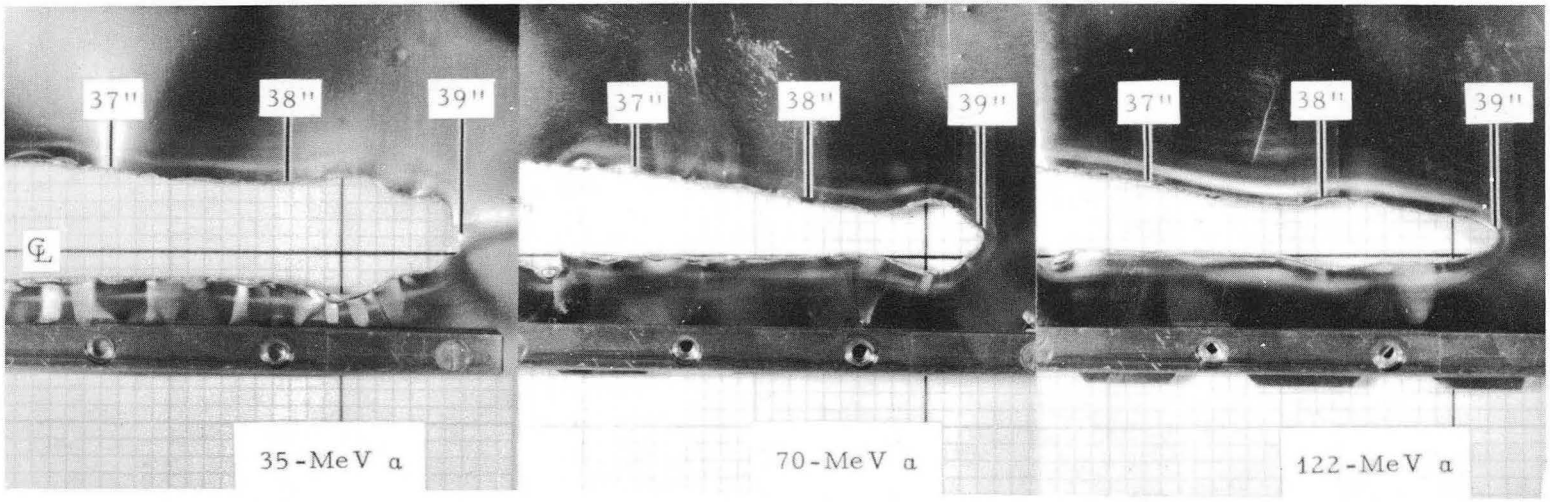

ZN-4331

Fig. 13. Internal beam profiles as shown by foil burns.

operation which permitted us to extract 100 μA of 32-MeV deuterons. Unfortunately, the copper septum leaked (for reasons other than beam bombardment) and had to be removed. Another copper septum is under construction and will be installed soon.

The 88-inch cyclotron runs 3 shifts a day, 7 days a week, with one shift for maintenance. The time distribution over the last 6 months is shown in Table I. As one can see from the table, there is about a 10% chance that an experimenter does not obtain the beam because of machine breakdown. It seems much more frequent to the experimenters involved! Tables II and III show the time distribution for two typical experiments as they are performed at the 88-inch cyclotron. Table II shows a scattering experiment extending over four consecutive shifts, and Table III shows isotope production of three different materials over two consecutive shifts. On the average, the beam is available for experiments about 80% of the scheduled time.

We are happy to acknowledge the contribution of Homer Conzett, who suggested a solid state detector as a phase probe; of Fred Goulding and Lloyd Robinson, who produced the crystals; and of Ronald Burger and Donald Elo, who designed the phase probe and assisted with the experiments.

This work was done under the auspices of the U. S. Atomic Energy Commission.

Table I. 88 Inch cyclotron time distribution, October 1963 through March 1964 (units of 8-hour shifts).

	Shifts	%
Physics (scattering)	268	48
Biophysics	18	3
Isotope production	130	23
Beam development	65	11
Preventive maintenance and changes	36	6
Repairs (lost scheduled time)	50	9
Total	567	100

Table II. Time distribution of a typical scattering experiment, running four consecutive shifts.

	Hours	%
Trim-coil change and tuning	2	6
Beam optics to chamber	4	12
Energy measurements	1/2	2
Beam for experiment	25-1/2	80
Total	32	100

Table III. Time distribution of two consecutive 8-hour shifts for three isotope-production targets of different energies.

	Hours	%
Three tuneups, trim-coil and gas change	3.75	23
Loading and unloading targets (concurrent with tuneups)	0	0
Beam on target	12.25	77
Total	16	100

1. Alper A. Garren and Lloyd Smith, Diagnosis and Correction of Beam Behavior in an Isochronous Cyclotron, UCRL-10756, April 1963.
2. H. E. Conzett, L. B. Robinson, and R. N. Burger, Semiconductor Probe for Investigating Accelerator Beam Pulses, Lawrence Radiation Laboratory Report UCRL-11492, June 1964.
3. Hermann A. Grunder, Frank B. Selph, and Hugo Atterling, Operating Experience with the Berkeley 88-Inch Cyclotron Electrostatic Deflector, UCRL-10759, April 1963.